J Ind Microbiol Biotechnol (2013) 40:1223–1229
DOI 10.1007/s10295-013-1330-2

BIOCATALYSIS

SIMB
Society for Industrial Microbiology and Biotechnology

Thermostabilization of *Bacillus subtilis* lipase A by minimizing the structural deformation caused by packing enhancement

Hong Seung Yun · Hyun June Park · Jeong Chan Joo · Young Je Yoo

Received: 1 February 2013 / Accepted: 6 August 2013 / Published online: 5 September 2013

Abstract Enzyme thermostabilization is a critical research topic due to potential industrial benefits. Among the various reasons to increase enzyme thermostability, enhancement of residual packing at the core of the enzyme structure has been commonly accepted as a successful strategy. However, structural changes that occur with residual packing enhancement may decrease enzyme activity. In this study, a strategy to minimize structural deformation by calculating the overlapping packing volume of a single-point mutation followed by applying a double-point mutation was suggested. Four double mutants, A38V_K23A, A75V_T83A, G80A_N106A, and G172A_V100A, were selected for the in vitro experiment; three of the four showed enhancements in both thermostability and catalytic activity. In particular, G80A_N106A showed 2.78 times higher catalytic activity compared with wild type.

Keywords Thermostabilization · Rational design · *Bacillus subtilis* lipase A · Residual packing enhancement

H. S. Yun · J. C. Joo · Y. J. Yoo (✉)
School of Chemical and Biological Engineering, Seoul National University, Seoul 151-742, Korea
e-mail: yjyoo@snu.ac.kr

H. J. Park · Y. J. Yoo
Graduate Program of Bioengineering, Seoul National University, Seoul 151-742, Korea

Y. J. Yoo
Bio-Max Institute, Seoul National University, Seoul 151-742, Korea

Introduction

Enzyme thermostabilization is an important issue in biotechnology research due to the potential benefits in industrial applications [8]. Despite recent progress in biotechnology, most critical bottlenecks involve protein stability. Numerous strategies have been developed to enhance protein thermostability [5, 7, 14, 20]. The rational design approach, which is efficient and in widespread use, identifies important factors that affect protein thermostability based on an understanding of their detailed structure and function [3, 11, 12]. Although some crystalline structures are unavailable, and it is often difficult to predict the effects of mutants, rational design is known for its cost efficiency and technical simplicity.

One rational strategy for enhancing protein thermostability is to enhance the residual packing of the protein interior. This strategy has been successfully applied to enzymes [13, 15, 18, 24]. The unfolding rate of enzymes can be reduced by replacing occluded and small hydrophobic residues with those that are more hydrophobic, thus enhancing hydrophobic interactions in the enzyme core. Our rational residual packing strategy yielded a dramatic increase in *Bacillus subtilis* lipase A thermostability, although mutants also exhibited a decrease in specific activity [1]. Industrial applications of enzyme biotechnology require the enhancement of both thermostability and catalytic activity, motivating further development of rational packing strategies.

In this study, a rational packing strategy was developed to achieve thermostability of the target enzyme *B. subtilis* lipase A by enhancing its residual packing while minimizing its structural deformation. Residual packing enhancement inevitably causes structural changes, including changes to catalytic sites, which may reduce or

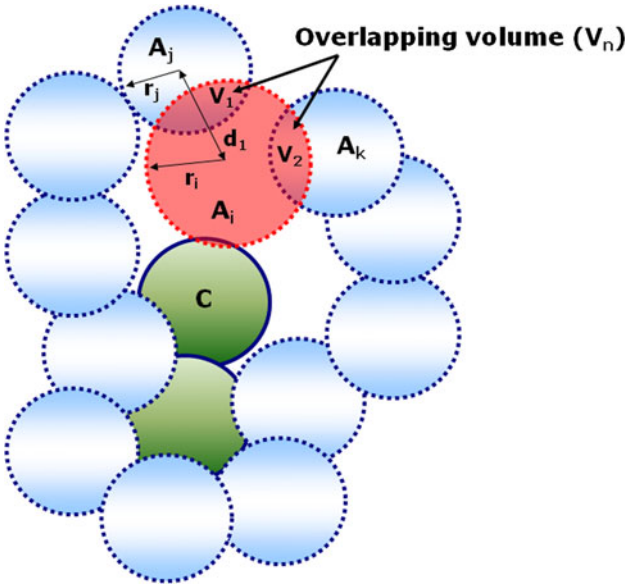

Fig. 1 Overlapping packing volume of single-point mutation. A_n imaginary atom, r_n radius of atom, d_n distance between atoms, V_n overlapping volume

eliminate catalytic activity. The key to maintaining stability, according to our approach, is to introduce other hydrophobic residues that result in minimal changes to the original structure. Previous approaches initially analyzed residual packing and residual exposure ratio to obtain reduced packing of glycine (Gly) or alanine (Ala) residues with no water contact. This produced minimal enhancement from residual packing. There are no smaller residues to replace the single-point mutation. Thus, mutating the neighboring residue to minimize the change in the original structure is desirable. Smaller amino acids are introduced after analyzing the overlapping packing volume of neighboring residues (Fig. 1). The overlapping packing volume of the target site is calculated using a simple equation. The degree of the structural change, upon mutation of the target sites, is estimated via computational design and calculation. Based on this information, target sites are mutated to achieve thermostable mutants with minimal structural change. After in vitro experiments using double-point mutations, an enzyme with enhanced activity and thermostability was successfully obtained.

Materials and methods

Computational design

Two *B. subtilis* lipase A structures, holo form 1I6W [23] and apo form 1R4Z [6], were used as a template for computational modeling. Their high-resolution Protein Data Bank (PDB) structure was used in this study. In silico mutations were designed by Discovery Studio and provided by Accelrys Inc., San Diego, CA, USA. Hydrogens were added to all PDB structures to improve calculation accuracy. All targeting candidates were designed using the following procedure: (1) calculation of the overlapping packing volume of single-point mutants and their neighboring residues, (2) selection of the target residue that most highly overlaps the neighboring residue's side chain, excluding residues that overlap at the polypeptide backbone, and (3) mutation of the selected residue using an amino acid with a smaller side chain (Ala). The distance between residues was also calculated with software provided by Discovery Studio.

Calculating the overlapping packing volume

The occluded and solvent-accessible surface area was calculated by an extension of the occluded surface algorithm and the Getarea 1.1 program, which was provided by the Sealy Center for Structural Biology at the University of Texas Medical Branch (Galveston Island, TX, USA) [9]. The occluded surface area indicates the degree of residual packing in contact with neighboring residues. The occluded surface area ratio equals 0.0 if the van der Waals surfaces of neighboring residues are located >2.8 Å of the molecular surface; the ratio equals 1.0 if the molecular surface is completely occluded by the van der Waals surface of other residues [16]. The exposure surface ratio indicates the ratio between the maximum surface area of the protein that can be in contact with a solvent molecule and takes into account the surface area of the solvent molecule; the exposure surface area equals 0.0 if there is no permitted contact area with the solvent and 100.0 if the molecular surface is fully exposed to solvent molecules. The default value for the solvent molecular radius is 1.4 Å.

The overlapping volume of two spheres can be calculated based on their Cartesian coordinates, in this case taken from the PDB crystalline structure. First, the coordinates of the two atoms must be projected to the *yz* plane, and one of them must be mapped onto the origin to simplify the rest of the equations. Equations 1 and 2 can then be formulated to describe the two spheres, where r_n indicates the radius of each atom, and d indicates the distance between the two atoms.

$$x^2 + y^2 + z^2 = r_1^2 \quad (1)$$

$$(x - d)^2 + y^2 + z^2 = r_2^2 \quad (2)$$

By combining and rearranging Eqs. 1 and 2, the x coordinate of the intersection of the two spheres can be expressed as shown in Eq. 3 by using the radius and the distance between the two spheres.

$$x = \left(d^2 - r_2^2 + r_1^2\right) / 2d \quad (3)$$

The sum of the two spherical caps, divided by the intersecting plane, can be considered as the overlapping volume of the two spheres. Cap heights (h_n) can be expressed as the difference in distance between the radius of each atom and the intersection (Eqs. 4, 5).

$$h_1 = r_1 - d_1 = \left[(r_2 - r_1 + d)\,(r_2 + r_1 - d)\right] / 2d \quad (4)$$

$$h_2 = r_2 - d_2 = \left[(r_1 - r_2 + d)\,(r_1 + r_2 - d)\right] / 2d \quad (5)$$

The volume of a spherical cap (Eq. 6) can be calculated as a function of the radius and the height.

$$V(r_n, h) = (1/3) \times \pi \times h_n^2 \times (3r_n - h_n) \quad (6)$$

Summing the two spherical caps gives Eq. 7.

$$\begin{aligned} V &= V(r_1, h_1) + V(r_2, h_2) \\ &= \Big[\pi \times (r_1 + r_2 - d)^2 \times \left(d^2 + 2dr_2 - 3r_2^2\right. \\ &\quad \left. + 2dr_1 + 6r_2 r_1 - 3r_1^2\right)\Big] / 12d \end{aligned} \quad (7)$$

The percentage of overlapping volume is therefore expressed as Eq. 8.

$$\left[V / \left(4\pi r_n^3 / 3\right)\right] \times 100\,(\%) \quad (8)$$

Site-directed mutagenesis

From the genomic DNA of *B. subtilis*, the lipase gene, *lipA*, was amplified and then cloned into the pET22b (+) vector (Novagen, Madison, WI, USA). The recombinant pET22b (+) vector was used as a template for both single and double mutants. Table 1 lists the primers used in this study. Site-directed mutagenesis was performed using *Pyrococcus furiosus* (Pfu) DNA polymerase and a thermal cycler [21]. DpnI endonuclease was used to digest or eliminate methylated template DNA. The mutated DNA was transformed into *Escherichia coli* DH5α by heat shock and plated onto an LB agar plate containing 50 μg/ml ampicillin. The transformed plate was incubated at 37 °C for 15 h. Single-bacterial colonies were then each transferred to 2 ml of Luria broth (LB) medium containing 50 μg/ml ampicillin and incubated at 37 °C overnight. The mutated plasmid DNA was purified using a plasmid DNA purification kit (RBC, Taipei, Taiwan) and verified by DNA sequencing (Cosmogentech, Seoul, Korea).

Table 1 Mutation primers for site-directed mutagenesis

Enzymes	Mutation primers
A38V_K23A	
A38V	F: 5′-CTGTATGTAGTTGATTTTTGGGAC-3′
	R: 5′-CAAAAATCAACTACATACAGCTTGTCCCG-3′
K23A	F: 5′-GGAATTGCGAGCTATCTCGTATCT-3′
	R: 5′-GATAGCTCGCAATTCCCGCAAAATTG-3′
A75V_T83A	
A75V	F: 5′-GATATTGTCGTTCACAGCATGGGGGGC-3′
	R: 5′-GCTGTGAACGACAATATCCACTTTTTTC-3′
T83A	F: 5′-GCGAACGCACTTTACTACATAAAAAATC-3′
	R: 5′-GTAAAGTGCGTTCGCGCCCCCCATG-3′
G80A_N106A	
G80A	F: 5′-CATGGGGGCCGCGAACACACTTTAC-3′
	R: 5′-GTTCGCGGCCCCCATGCTGTGAGC-3′
N106A	F: 5′-GGCGCGGCCCGTTTGACGACAGGC-3′
	R: 5′-CAAACGGGCCGCGCCGCCCAGCGTC-3′
G172A_V100A	
G172A	F: 5′-GATTAAAGAAGCGCTGAACGGCGGGGGC-3′
	R: 5′-GTTCAGCGCTTCTTTAATCAGGCTG-3′
V100A	F: 5′-CAAACGTCGCGACGCTGGGCGGCGCG-3′
	R: 5′-CAGCGTCGCGACGTTTGCAACTTTATTTC-3′

Protein expression and purification

One hundred milliliters of LB medium with 50 μl of ampicillin was inoculated with 5 ml of *E. coli* BL21 (DE3) containing the recombinant lip A pET22b (+) plasmid. The culture was incubated at 37 °C with shaking until the optical density measured at a wavelength of 600 nm (OD600) reached; 0.5–0.7. 2 % (v/v) of isopropyl-β-thio-galactopyranoside was then added to induce recombinant lipase A expression, and the culture was incubated at 20 °C for 24 h. The transformed cells were then harvested by centrifugation and resuspended in 40 ml of lysis buffer [50 mM sodium phosphate (NaH_2PO_4), 300 mM sodium chloride (NaCl), and 10 mM imidazole; pH 8.0). After sonication for 10 min, cell debris was removed by centrifugation to isolate the supernatant containing soluble recombinant lipase. One milliliter of nickel-nitrilotriacetic acid (Ni–NTA) agarose beads (Qiagen, Hilden, Germany) was added to the supernatant, followed by gentle mixing at 4 °C for 1 h. After washing eight times with 5 ml of wash buffer (50 mM NaH_2PO_4, 300 mM NaCl, and 20 mM imidazole; pH 8.0), the bound proteins were eluted four times with 0.5 ml of elution buffer (50 mM NaH_2PO_4, 300 mM NaCl, and 250 mM imidazole; pH 8.0). After elution, the sample solution was subjected to centrifugal ultrafiltration using an Amicon Ultra-15 centrifugal filter of 10 normal molecular weight limit (NMWL) (Millipore, MA, USA) to remove imidazole, which participates in side reactions and hydrolyzes p-nitrophenyl caprylate (pNPC, Sigma-Aldrich, MO, USA), a component in the lipase assay. Purified enzymes in phosphate buffer (50 mM NaH_2PO_4 and 300 mM NaCl; pH 8.0) were confirmed by 12 % sodium dodecyl sulfate polyacrylamide gel electrophoresis (SDS-PAGE). The enzyme concentration was

determined using a modified Bradford assay (Sigma-Aldrich) following the manufacturer's instructions.

Measurement of specific activity and thermostability

The lipase activity assay was conducted using a modification of Gupta's method [10]: pNPC dissolved in acetonitrile (33.3 mM) was mixed with the reaction buffer (pH 8.0, 50 mM phosphate buffer, and 0.5 % Triton X) (Sigma-Aldrich) and enzyme solution (10 μg/ml), to a total volume of 1,000 μl and a substrate/enzyme/reaction buffer volume ratio of 90:100:810. pNPC was used as a standard substrate (final concentration 3 mM) because lipA is the most active toward pNPC compared with other types of *p*-nitrophenyl esters. The substrate was added to the reaction buffer and mixed by vortexing. As soon as the enzyme solution was added to the mixed substrate solution, absorbance was measured at 405 nm for 3 min at 30 °C using a Cary 50 UV spectrophotometer (Varian, Palo Alto, CA, USA). Initial lipA reaction rate was determined from the slope of absorbance over time. Thermostability was determined by measuring the residual activity of lipA variants after incubation at 35 °C for 1 h. All experimental values are presented as the average of triplicate measurements.

Results and Discussion

Target-site selection

The six single mutations made in a previous study (A38V, A75V, G80A, A105V, A146V, and G172A) [1] were used as a template for the double mutant. However, among the six single mutants, A105V and A146V were excluded because these residues play an important role in the formation of the hydrophobic interaction network. Ala 105 interacts with Ser 77, Met 78, Leu 108, Val 136, and Leu 140. Among the five interacting residues, all except Ser 77 are hydrophobic residues that interact with several other hydrophobic residues to form a hydrophobic network at the core of the enzyme. Moreover, Ser 77 is a catalytic residue, the mutation of which may decrease catalytic activity. Ala 146 interacts with Ala 113, Tyr 125, Thr 126, Ser 127, Leu 143, and Gln 178. These interactions constitute the polypeptide backbone and involve many atoms. Mutation of the residues that interact with many atoms could result in severe structural changes, including changes to the structure of the catalytic sites, which would cause the loss of catalytic activity. Furthermore, Ala 113, Tyr 125, and Leu 143 play an important role in the hydrophobic interaction network. Weakening hydrophobic interaction may decrease protein thermostability.

Selection of target site for A38V variant

In the case of A38V, the overlapping residues are Met 8, Ser 16, Phe 19, and Lys 23 (Table 2). The residue with the largest overlapping volume is Lys 23, located at the side chain. This residue was selected for further study. Phe 19 was excluded because of its many interactions with other residues, comprising five hydrophobic interactions, one aromatic-sulfur interaction, and two hydrogen bonds linking segments of the main chain. Disruption of these types of interactions may accelerate the rate of unfolding and decrease protein thermostability. The same rationale was used to exclude Met 8, which participates in hydrophobic interactions and hydrogen bonding between segments of the main chain. However, its location at the polypeptide backbone indicated that mutation of this residue may cause significant structural change. Therefore, Ser 16 was excluded from mutation.

Selection of target site for A75V variant

Residues that overlap with A75V are Val 9, Gly 79, Gly 80, Thr 83, and Thr 101 (Table 3). Because of a higher overlapping packing percentage at the side chain, Thr 83 was selected as a target for double-point mutation. Both Gly 79

Table 2 Percentage of overlapping volume within 6 **Å** for A38V variant

Residue	Atom	*x*	*y*	*z*	Percentage
Met 8	CB	−13.566	23.078	11.034	10.578
Ser 16	CB	−18.531	18.434	8.720	32.988
Ser 16	O	−19.332	21.360	9.796	15.365
Ser 16	CA	−18.924	19.012	10.083	26.019
Ser 16	C	−19.817	20.233	9.881	19.018
Phe 19	CD2	−16.838	22.527	12.537	9.183
Phe 19	CB	−17.603	24.423	11.068	5.587
Lys 23	NZ	−16.817	22.949	5.903	16.157
Lys 23	CE	−16.407	24.117	6.724	21.349

Table 3 Percentage of overlapping volume within 6 **Å** for A75V variant

Residue	Atom	*x*	*y*	*z*	Percentage
Val 9	CB	−11.483	19.125	14.777	13.686
Gly 79	O	−9.957	18.363	18.766	18.028
Gly 79	C	−10.959	18.67	19.414	33.572
Gly 80	N	−10.924	19.493	20.462	17.375
Gly 80	C	−8.764	18.958	21.457	5.042
Thr 83	OG1	−8.001	19.152	16.834	18.079
Thr 83	CB	−6.827	19.061	17.649	15.676
Thr 101	CG2	−8.049	24.037	20.637	9.144

and Gly 80 were excluded because their backbone overlapped with the imaginary sphere. Val 9 and Thr 101 play an important role in hydrophobic networks.

Selection of target site for G80A variant

As shown in Table 4, residues that overlap with G80A are Ser 77, Gly 79, Ala 81, Thr 101, and Asn 106. Ser 77 was rejected as a candidate because it is one of the residues in the catalytic triad. Gly 79 and Ala 81 were excluded because the imaginary sphere overlapped with the backbone of these residues. Thr 101 was excluded because the percentage of overlapping volume was negligible. Therefore, Asn 106 was selected as a target residue for the double mutant.

Selection of target site for G172A variant

G172A, which is different from the other cases, overlaps with Val 100, Thr 126, Glu 171, and Leu 173 (Table 5). Previous cases excluded interacting residues based on several criteria. However, the overlap between G172A and these residues was negligible, with the exception of Val 100; thus, Val 100 was selected for further research.

Comparison of thermostability and catalytic activity of double mutants

In vitro mutagenesis was used to create four double mutants: A38V_K23A, A75V_T83A, G80A_N106A, and G172A_V100A. To analyze enzyme thermostability, their relative activity was compared after 1 h of incubation at 35 °C. As shown in Fig. 2, thermostability of A38V_K23A, G80A_N106A, and G172A_V100A variants increased 1.95-, 1.37-, and 1.47-fold, respectively. However, the A75V_T83A variant exhibited a decrease in thermostability to 75 % of its initial activity. The increasing thermostability of the variants can be explained by packing enhancement at the core of the enzyme. The residual packing was enhanced by replacing large hydrophobic residues with smaller residues via single-point mutation and performing double-point mutations on the neighboring residues so that the volume of the mutated residues was equal to the side chain of the target.

To analyze the relative activity of lipase A, its catalytic activity was measured via enzyme kinetics. By plotting the Lineweaver–Burk plot, kinetic parameters such as V_m, K_m, and k_{cat} were calculated by rearranging the Michaelis–Menten equation (Table 6). The variants exhibited lower V_m values, which is the theoretical maximal rate of reaction. Although k_{cat} decreased, K_m also decreased. Catalytic activity (k_{cat}/K_m) of all variants showed an increase of between 1.60- and 2.78-fold (Fig. 2) compared with wild type.

Whereas core-packing enhancement stabilizes hydrophobic interactions and enhances enzyme thermostability, it also accompanies a loss of the enzyme's catalytic

Table 4 Percentage of overlapping volume within 6 Å for G80A variant

Residue	Atom	*x*	*y*	*z*	Percentage
Ser 77	O	−12.943	19.917	22.528	0.022
Gly 79	C	−10.959	18.670	19.414	0.030
Ala 81	N	−9.349	18.037	22.220	0.634
Thr 101	CG2	−8.049	24.037	20.637	0.005
Asn 106	OD1	−8.415	21.746	23.595	8.477
Asn 106	CG	−7.937	22.302	24.585	1.344

Table 5 Percentage of overlapping volume within 6 Å for G172A variant

Residue	Atom	*x*	*y*	*z*	Percentage
Val 100	CG2	−7.288	29.621	16.151	15.443
Val 100	CB	−8.319	28.692	16.785	0.009
Thr 126	OG1	−4.754	31.977	19.149	0.157
Thr 126	CB	−5.809	31.216	19.746	0.230
Glu 171	C	−5.968	35.519	15.110	0.040
Lue 173	N	−6.078	32.682	13.286	0.656

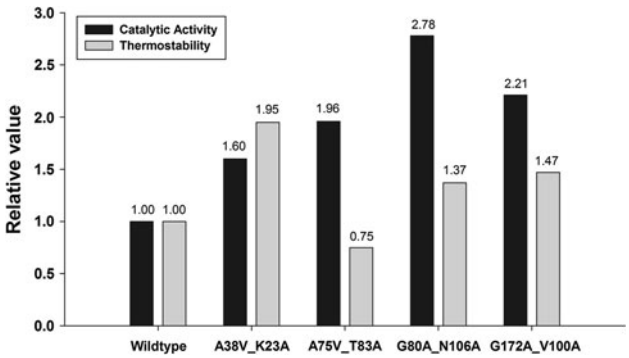

Fig. 2 Comparison of catalytic activity and thermostability of *Bacillus subtilis* lipase A variants. *Numbers above the bars* represent relative value of each bar

Table 6 Kinetic parameter data of *Bacillus subtilis* lipase A variants

Enzyme	V_m (μm/min)	K_m (μM)	k_{cat} (1/min)	k_{cat}/K_m (1/μM/min)
Wild type	196.078	21.765	7.594	0.349
A38V_K23A	82.645	6.851	3.828	0.559
A75V_T83A	45.249	2.010	1.376	0.685
G80A_N106A	70.423	6.908	6.711	0.971
G172A_V100A	29.851	1.907	1.476	0.773

activity. One putative explanation is that the rigidity of the enzyme increases when residual packing of its interior is enhanced; because an enzyme's function depends on its conformational change, such a decrease in flexible motion might reduce its activity. With the exception of A75V_T83A, packing-enhanced variants were more thermostable than the wild type. Although A75V_T83A was destabilized by packing enhancement, it still retained 75 % of its initial activity after incubation at 35 °C for 1 h. Interestingly, catalytic activity of all variants increased upon applying the rational packing strategy suggested in this study. The substrate-binding affinity of the variants dramatically increased, even though their turnover number simultaneously decreased; therefore, overall catalytic activity of the variants was higher than the wild type in all cases. Because activity and stability of both wild type and mutant *B. subtilis* lipase A show the same trends at different temperatures [2, 4, 17], our strategy may also be applied over a wider range of temperatures than those used in this study.

In silico analysis of activity enhancement

Our strategy aimed to preserve wild-type catalytic activity by minimizing structural deformation of the enzyme while enhancing residual packing at its core. Introducing a residue such as Ala, which is smaller than the target residue, also introduces the possibility of decreasing the packing. The increase in relative catalytic activity for all variants was unexpected. Hence, modeling of variant structures was performed via energy minimization to elucidate the relationship between catalytic activity and relevant structural features, which in the case of *B. subtilis* lipase A are the catalytic triad and the oxyanion hole [19, 22]. Analysis of the *B. subtilis* lipase A crystal structure identifies that the catalytic triad (Ser 77, Asp 133, and His 156) and the oxyanion hole (Ile 12 and Met 78) are involved in catalytic motion, where Ser and His are directly involved and Asp is essential for stabilizing the transition state. The direct involvement of Ser and His is inferred from ab initio quantum mechanics/molecular mechanics (QM/MM) analysis of another esterase [19]. The oxyanion hole, formed by two peptidic NH groups from isoleucine and methionine, stabilizes high-energy intermediates and the transition state by forming hydrogen bonds to the ester group of the substrate. Residues forming the catalytic triad and the oxyanion hole are connected by several hydrogen bonds, as shown in Figs. 3 and 4. These hydrogen bonds are important in the catalytic reaction because the transfer of protons and electrons depends on the distance between catalytic residues. Therefore, catalytic activity may change with mutations that form or break hydrogen bonds or that change their distance from the catalytic triad and oxyanion hole (Table 7).

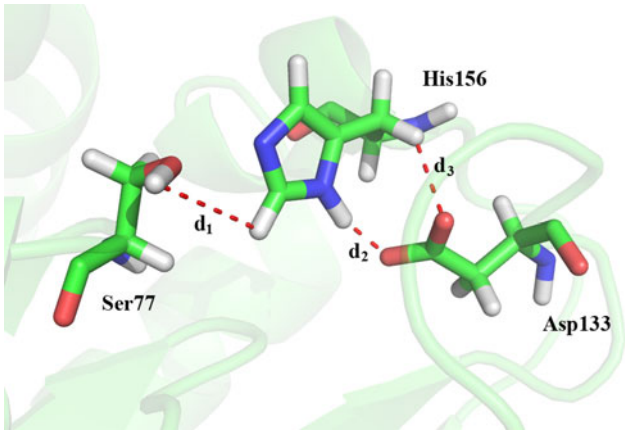

Fig. 3 Catalytic triad of *Bacillus subtilis* lipase A (1I6W). d_1 Distance between Ser 77 and His 156, d_2 and d_3 distance between His 156 and Asp 133, *white atom* hydrogen, *red atom* nitrogen, *blue atom* oxygen, *green atom* carbon (color figure online)

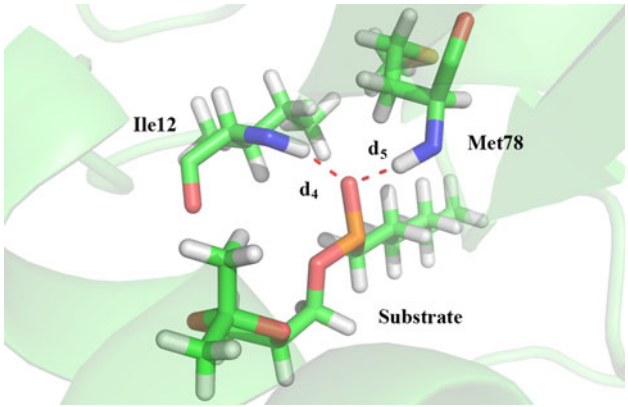

Fig. 4 Substrate and oxyanion hole of *Bacillus subtilis* lipase A (1R4Z). d_4 Distance between Ile 12 and substrate, d_5 distance between Met 78 and substrate, *white atom* hydrogen, *red atom* nitrogen, *blue atom* oxygen, *green atom* carbon, *orange atom* sulfur (color figure online)

Table 7 Distances of hydrogen bonds between catalytic residues and oxyanion hole

	d_1 (Å)	d_2 (Å)	d_3 (Å)	d_4 (Å)	d_5 (Å)
Wild type	4.092	2.046	4.097	2.016	2.255
A38V_K23A	4.265	2.094	3.949	1.888	2.050
A75V_T83A	3.439	1.917	3.907	2.024	1.955
G80A_N106A	3.985	2.121	4.405	2.152	2.144
G172A_V100A	3.991	2.011	4.428	2.221	2.258

In the case of the three hydrogen bonds (d_1, d_2, and d_3) forming the catalytic triad, d_1 and d_3 showed differences in distance between the wild type and variants; however, d_2 in variants showed only a slight difference of <5 % compared

with the wild type. The d_1 of the A75V_T83A variant was shorter relative to its value than the wild type; in contrast, the d_3 of G80A_N106A and G172A_V100A was longer relative to the d_3 of the wild type. No significant trend was observed in the catalytic activity that was observed with regard to the distance of hydrogen bonds. In the case of the two hydrogen bonds forming the oxyanion hole (d_4 and d_5), the variants showed no significant difference compared with the wild type. Although d_5 values of variants were slightly shorter than that of the wild type, this difference was not sufficient to explain the effect of the mutation on catalytic activity.

Conclusion

This study presents a new mutation strategy to enhance enzyme thermostability while maintaining its catalytic activity by minimizing the structural deformation that typically occurs during mutations that increase residual packing in the enzyme core. The strategy is based on double-point mutations, where the overlapping packing volume of a single-point mutation is calculated, and a second-point mutation is performed so that the total packing volume of the mutated residues is equal to that of the original residue's side chain, thus stabilizing the structure. All four mutants exhibited higher catalytic activity than the wild type, particularly G80A_N106A. In silico analysis revealed slight changes in the distance between several hydrogen bonds and the catalytic triad or oxyanion hole, and these changes may affect both substrate-binding affinity and catalytic efficiency. This proposed strategy has broad applications toward all types of enzymes in industrial applications.

Acknowledgments This work was supported by the National Research Foundation of Korea Grant funded by the Korean Government (MEST) (NRF-2009-C1AAA001-2009-0093512).

References

1. Abraham T, Pack SP, Je Yoo Y (2005) Stabilization of *Bacillus subtilis* lipase A by increasing the residual packing. Biocatal Biotransformation 23(3–4):217–224. doi:10.1080/10242420500193013
2. Ahmad S, Rao NM (2009) Thermally denatured state determines refolding in lipase: mutational analysis. Protein Sci 18(6):1183–1196
3. Böttcher D, Bornscheuer UT (2010) Protein engineering of microbial enzymes. Curr Opin Microbiol 13(3):274–282. doi:10.1016/j.mib.2010.01.010
4. Boersma YL, Pijning T, Bosma MS, van der Sloot AM, Godinho LF, Dröge MJ, Winter RT, van Pouderoyen G, Dijkstra BW, Quax WJ (2008) Loop grafting of *Bacillus subtilis* lipase A: inversion of enantioselectivity. Chem Biol 15(8):782–789
5. Bornscheuer UT, Pohl M (2001) Improved biocatalysts by directed evolution and rational protein design. Curr Opin Chem Biol 5(2):137–143. doi:10.1016/S1367-5931(00)00182-4
6. Dröge MJ, Boersma YL, Van Pouderoyen G, Vrenken TE, Rüggeberg CJ, Reetz MT, Dijkstra BW, Quax WJ (2006) Directed evolution of *Bacillus subtilis* lipase A by use of enantiomeric phosphonate inhibitors: crystal structures and phage display selection. ChemBioChem 7(1):149–157. doi:10.1002/cbic.200500308
7. Eijsink VGH, GÅseidnes S, Borchert TV, Van Den Burg B (2005) Directed evolution of enzyme stability. Biomol Eng 22(1–3):21–30. doi:10.1016/j.bioeng.2004.12.003
8. Fagain CO (1995) Understanding and increasing protein stability. Biochim et Biophys Acta Protein Struct Mol Enzymol 1252(1):1–14. doi:10.1016/0167-4838(95)00133-F
9. Fraczkiewicz R, Braun W (1998) Exact and efficient analytical calculation of the accessible surface areas and their gradients for macromolecules. J Comput Chem 19(3):319–333
10. Gupta N, Rathi P, Gupta R (2002) Simplified para-nitrophenyl palmitate assay for lipases and esterases. Anal Biochem 311(1):98–99. doi:10.1016/S0003-2697(02)00379-2
11. Kim HS, Le QAT, Kim YH (2010) Development of thermostable lipase B from *Candida antarctica* (CalB) through in silico design employing B-factor and RosettaDesign. Enzym Microb Technol 47(1–2):1–5. doi:10.1016/j.enzmictec.2010.04.003
12. Kim SJ, Lee JA, Joo JC, Yoo YJ, Kim YH, Song BK (2010) The development of a thermostable CiP (*Coprinus cinereus* peroxidase) through in silico design. Biotechnol Prog 26(4):1038–1046. doi:10.1002/btpr.408
13. Lim WA, Sauer RT (1991) The role of internal packing interactions in determining the structure and stability of a protein. J Mol Biol 219(2):359–376
14. Pack SP, Yoo YJ (2004) Protein thermostability: structure-based difference of amino acid between thermophilic and mesophilic proteins. J Biotechnol 111(3):269–277. doi:10.1016/j.jbiotec.2004.01.018
15. Pack SP, Yoo YJ (2005) Packing-based difference of structural features between thermophilic and mesophilic proteins. Int J Biol Macromol 35(3–4):169–174. doi:10.1016/j.ijbiomac.2005.01.007
16. Pattabiraman N, Ward KB, Fleming PJ (1995) Occluded molecular surface: analysis of protein packing. J Mol Recognit 8(6):334–344
17. Reetz MT, Carballeira JD, Vogel A (2006) Iterative saturation mutagenesis on the basis of b factors as a strategy for increasing protein thermostability. Angewandte Chemie Int Ed 45(46):7745–7751
18. Sandberg WS, Terwilliger TC (1989) Influence of interior packing and hydrophobicity on the stability of a protein. Science 245(4913):54–57
19. Schmid RD, Verger R (1998) Lipases: interfacial enzymes with attractive applications. Angewandte Chemie Int Ed 37(12):1609–1633
20. Steipe B (1999) Evolutionary approaches to protein engineering. Curr Top Microbiol Immunol 243:55–86
21. Trodler P, Nieveler J, Rusnak M, Schmid RD, Pleiss J (2008) Rational design of a new one-step purification strategy for *Candida antarctica* lipase B by ion-exchange chromatography. J Chromatogr A 1179(2):161–167. doi:10.1016/j.chroma.2007.11.108
22. Uppenberg J, Öhrner N, Norin M, Hult K, Kleywegt GJ, Patkar S, Waagen V, Anthonsen T, Alwyn Jones T (1995) Crystallographic and molecular-modeling studies of lipase B from *Candida antarctica* reveal a stereospecificity pocket for secondary alcohols. Biochemistry 34(51):16838–16851
23. Van Pouderoyen G, Eggert T, Jaeger KE, Dijkstra BW (2001) The crystal structure of *Bacillus subtilis* lipase: a minimal α/β hydrolase fold enzyme. J Mol Biol 309(1):215–226. doi:10.1006/jmbi.2001.4659
24. Vlassi M, Cesareni G, Kokkinidis M (1999) A correlation between the loss of hydrophobic core packing interactions and protein stability. J Mol Biol 285(2):817–827. doi:10.1006/jmbi.1998.2342